JOURNAL OF GUIDANCE, CONTROL, AND DYNAMICS
Vol. 32, No. 5, September–October 2009

Engineering Notes

Multibody Model of an Ornithopter

Jared A. Grauer* and James E. Hubbard Jr.†
University of Maryland, College Park, Maryland 20742

DOI: 10.2514/1.43177

I. Introduction

MINIATURE ornithoptic aircraft are receiving growing attention from hobbyists and researchers as interest in promising new vehicle designs, made possible by miniaturizations in electronics and improvements in materials manufacturing, synergizes with inspiration from winged creatures in nature. It is envisioned that the agility, maneuverability, robustness, and contextual camouflage exhibited by these avian-inspired robots will fill a niche left open by conventional fixed and rotating wing aircraft in the quest for autonomous flight vehicles which integrate multimission capabilities such as perch and stare maneuvers, flight through cluttered indoor environments, and long endurance flight.

Vital to the achievement of these goals is the development of an accurate flight dynamics model, which constitutes a significant challenge due to the complex aerodynamic flowfields, variable inertial properties, and highly nonlinear motions which characterize ornithoptic flight. Although the aerodynamic modeling of flapping wings remains an open research problem, ongoing developments in recent years using both analytical blade element methods [1–3] and computational fluid dynamics [4–6] have shed light on the principle aerodynamic phenomenon that enables flapping flight. Recent studies in insect and micro air vehicle flight dynamics have applied these aerodynamic models to the conventional equations of a rigid body aircraft for the purposes of simulation and control [7–9]. As the vehicle size is increased to meet payload requirements and to reduce wind gust sensitivity, the wings become increasingly massive and flap at lower frequencies, which requires multibody models to describe the changing mass distribution and coupling effects between moving aircraft components [10,11].

The focus of this work is to develop the nonlinear multibody flight dynamics of an ornithopter and cast the equations into a canonical form that is convenient to perform the system identification, nonlinear controller synthesis, and simulation case studies required to realize an autonomous ornithopter. First, an ornithopter research platform is introduced and observations of the flight dynamics and mass properties warranting a nonlinear multibody model are discussed. Although centered around a particular ornithopter, the model presented in this paper is easily extended to describe other aircraft configurations, actuation methods, and aerodynamic models. Second, the ornithopter is posed as a multibody problem, after which the equations of motion are derived using energy methods and are molded into a canonical form. Lastly, a simplified aerodynamics model is used to perform a realistic simulation which illustrates the trends observed in flight data and strengthens arguments for using a nonlinear multibody model.

Presented as Paper 727 at the 47th AIAA Aerospace Sciences Meeting including The New Horizons Forum and Aerospace Exposition, Orlando, FL, 5–8 January 2009; received 11 January 2009; revision received 1 June 2009; accepted for publication 5 June 2009. Copyright © 2009 by the American Institute of Aeronautics and Astronautics, Inc. All rights reserved. Copies of this paper may be made for personal or internal use, on condition that the copier pay the $10.00 per-copy fee to the Copyright Clearance Center, Inc., 222 Rosewood Drive, Danvers, MA 01923; include the code 0731-5090/09 and $10.00 in correspondence with the CCC.

*Graduate Student, Department of Aerospace Engineering. Member AIAA.

†Langley Distinguished Professor, Department of Aerospace Engineering. Associate Fellow AIAA.

II. Ornithopter Test Aircraft

The ornithopter about which the modeling is centered is a modified version of the "Slow Hawk" Kinkade ornithopter [12], shown in Fig. 1, which has a wingspan of 1.2192 m and a mass of 0.4460 kg. The vehicle is flown remotely by a pilot using standard hobby radio equipment. One joystick commands the speed of a dc motor, which through a gear box and a four-bar linkage flaps the wings in unison to generate lift and thrust. A second joystick is used to command two servomotors, which pitch and roll linkages in a serial manner to deflect the tail and generate aerodynamic control forces.

Unlike conventional aircraft, an ornithopter experiences significant and rapid changes in the mass distribution during flight due to the flapping of the wings and the positioning of the tail. Mass properties were measured by partitioning the ornithopter into five rigid bodies and measuring the mass properties of the composite components. The fuselage comprises 76% of the total vehicle mass, followed by the wings with 19%, and the tail linkages with 5%. Figure 2 illustrates the dramatic changes in the vertical position of the center of mass and the pitching and yawing moments of inertia of the entire vehicle as the wings change position, where the vehicle inertia is resolved about the vehicle center of mass, which is given relative to the stationary fuselage center of mass.

The ornithopter is physically constructed as a multibody system and requires a multibody model to accurately account for the configuration-dependent inertial properties. Additionally, previous work [13] has reported that this ornithopter flaps at 4.7 Hz and experiences pitch rates of 5.62 rad/s and heave accelerations of 46.1 m/s^2 in straight and level mean flight, which indicates that a multibody model should be used to capture the fast motions and the interactions of the wings flapping with the rest of the system. Additionally a multibody model is convenient for resolving aerodynamic forces, as the body configuration and velocities are state variables within the model.

III. Model Configuration

The ornithopter is modeled as a system of five rigid bodies, consisting of three chains emanating in a tree structure from a central fuselage body, as shown in Fig. 3. Each linkage i on chain j has mass m_{ij} and inertia tensor $\mathbf{I}_{ij}$ about center of mass C_{ij} and reference frame K_{ij}. Vectors $\mathbf{l}ij$ and $\mathbf{r}_{ij}$ describe the positions of the inboard and outboard revolute joint locations, which rotate about axes $\mathbf{z}_{ij}$ and $\mathbf{z}_{(i+1)j}$, respectively. The first two kinematic chains are the right and left wings, which rotate about the longitudinal axis of the fuselage. The third chain comprises the tail mechanism, which collectively pitches and rolls about the fuselage through two linkages. Additionally an inertial reference C_I, K_I is taken at a fixed point on the surface of the Earth.

The fuselage, body 0, has an inertial position $\mathbf{r}$ and an orientation quaternion $\boldsymbol{\eta}$ which are expressed in the inertial frame K_I. The translational and rotational velocities of the fuselage are $\boldsymbol{\nu}$ and $\boldsymbol{\omega}$, and are expressed in the fuselage frame K_0. The attached linkages have angular positions $\boldsymbol{\theta} = [\theta_{11}, \theta_{12}, \theta_{13}, \theta_{23}]^T$ and angular velocities $\dot{\boldsymbol{\theta}}$ which are expressed in their respective reference frames. This choice of position and velocity states parallels the conventional aircraft equations, provides a compact formulation of the dynamics, and forms the equations of motion in the same reference frames in which sensor measurements are taken and control forces are applied.

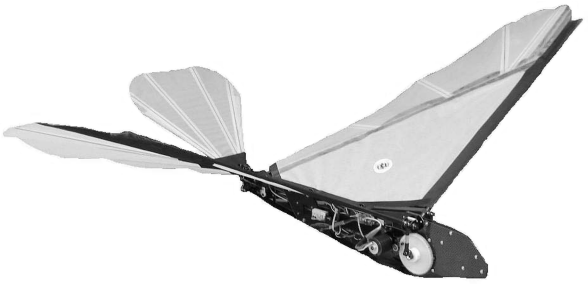

Fig. 1 Ornithopter research platform [13].

Using the configuration of the system and the body-fixed geometric vectors, the position and velocity of link *i* of chain *j* can be written

$$\mathbf{r}_{ij} = \mathbf{r} + \mathbf{r}_{0j} + \sum_{k=1}^{i-1}(\mathbf{r}_{kj} - \mathbf{l}_{kj}) - \mathbf{l}_{ij} \tag{1}$$

$$\boldsymbol{\omega}_{ij} = \boldsymbol{\omega} + \sum_{k=1}^{i} \dot{\theta}_{kj}\mathbf{z}_{kj} \tag{2}$$

$$\boldsymbol{v}_{ij} = \boldsymbol{v} + \mathbf{S}(\boldsymbol{\omega})\mathbf{r}_{0j} + \sum_{k=1}^{i-1}\mathbf{S}(\boldsymbol{\omega}_{kj})(\mathbf{r}_{kj} - \mathbf{l}_{kj}) - \mathbf{S}(\boldsymbol{\omega}_{ij})\mathbf{l}_{ij} \tag{3}$$

where $\mathbf{S}(\cdot)$ denotes the matrix implementation of the cross- product operation.

IV. Equations of Motion

The equations of motion are differential equations which describe the evolution of the state variables in time. The generalized position states are the position and orientation of the fuselage and the joint angle vector, and the generalized velocity states are the translational and rotational velocities of the fuselage and the joint rate vector:

$$\mathbf{p} = [\,\mathbf{r}^T \quad \boldsymbol{\eta}^T \quad \boldsymbol{\theta}^T\,]^T \tag{4}$$

$$\mathbf{v} = [\,\boldsymbol{v}^T \quad \boldsymbol{\omega}^T \quad \dot{\boldsymbol{\theta}}^T\,]^T \tag{5}$$

The kinematic equations relate the derivatives of the position states to the velocity states and are written

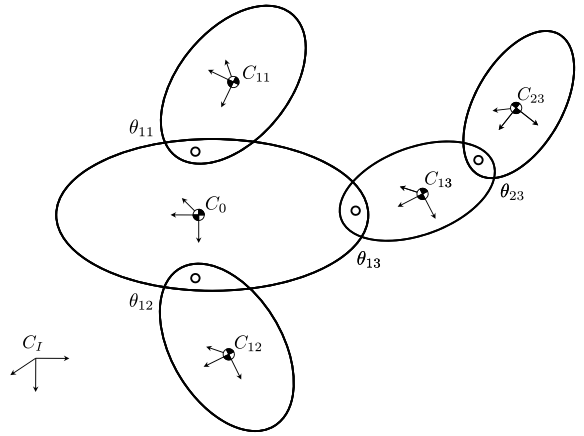

Fig. 3 Multibody representation of the ornithopter.

$$\dot{\mathbf{p}} = \mathbf{J}_K^{I,0}\mathbf{v} \tag{6}$$

where the matrix $\mathbf{J}_K^{I,0}$ is dependent on the fuselage orientation and has along the diagonal a rotation matrix, an orientation Jacobian matrix, and an identity matrix.

The dynamic equations of motion describe the evolution of the velocity states as a function of the applied forces and torques on the system. The Boltzmann–Hamel equations are employed in this work, which are based on energy functions and allow for state variables to be expressed in different reference frames. Although numerous differentiations of the energy functions are required, the calculations are procedural and can easily be implemented in symbolic algebra software packages. Additionally the analysis results in a minimal number of state equations and the energy functions may be used as inspiration for the design of nonlinear control laws [14]. The kinetic energy of the ornithopter is

$$T = \frac{1}{2}\sum_{j=0}^{3}\sum_{i=0}^{2} m_{ij}\boldsymbol{v}_{ij}^T\boldsymbol{v}_{ij} + \boldsymbol{\omega}_{ij}^T\mathbf{I}_{ij}\boldsymbol{\omega}_{ij} \tag{7}$$

which combines the translational and rotational energies of the fuselage and linkages. The Boltzmann–Hamel equations are

$$\frac{\mathrm{d}}{\mathrm{d}t}\left[\frac{\partial T}{\partial \mathbf{v}}\right]^T + \left(\sum_{k=1}^{N}\left[\frac{\partial T}{\partial v_k}\right]\Gamma_k\right)\mathbf{v} - (\mathbf{J}_K^{I,0})^T\left[\frac{\partial T}{\partial \mathbf{p}}\right]^T = \boldsymbol{\tau} \tag{8}$$

where $\boldsymbol{\tau}$ represents a vector of generalized forces and torques acting on the velocity states, and where

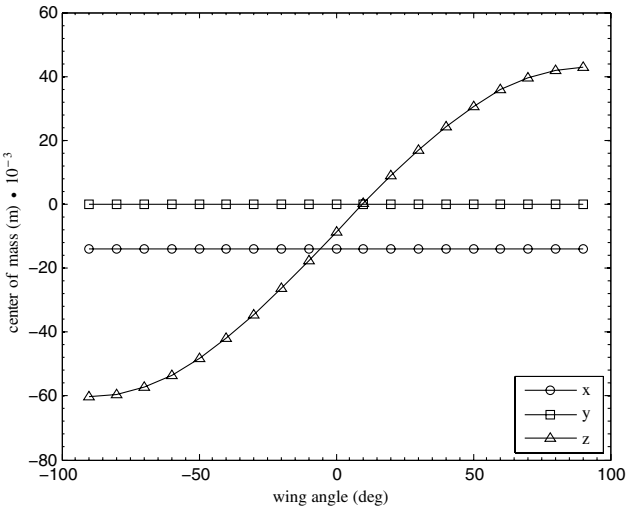

a) Center of mass

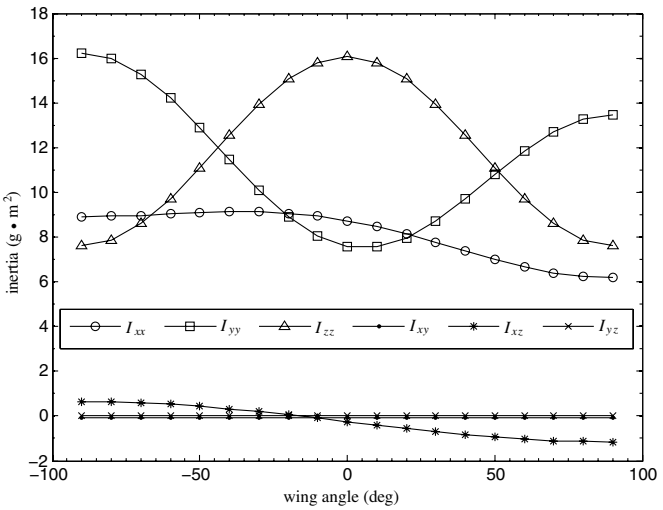

b) Inertia tensor

Fig. 2 Variation of the gross mass distribution with wing position.

$$\Gamma_k = (\mathbf{J}_K^{I,0})^T \mathbf{\Lambda}_k (\mathbf{J}_K^{I,0}) \tag{9}$$

with matrix entries

$$\{\mathbf{\Lambda}_k\}_{ij} = \frac{\partial}{\partial p_j}\{\mathbf{J}_K^{0,I}\}_{ki} - \frac{\partial}{\partial p_i}\{\mathbf{J}_K^{0,I}\}_{kj} \tag{10}$$

After some manipulation, the dynamic equations of motion may be partitioned as

$$\mathbf{M}(\mathbf{p})\dot{\mathbf{v}} + \mathbf{C}(\mathbf{p},\mathbf{v})\mathbf{v} + \mathbf{E}(\mathbf{p},\mathbf{v}) = \boldsymbol{\tau} \tag{11}$$

which is a canonical form for the nonlinear control of mechanical systems such as spacecraft and robot manipulators [15]. The matrix $\mathbf{M}(\mathbf{p})$ describes the generalized mass and inertia properties of the system and is dependent upon the joint angles. The matrix $\mathbf{C}(\mathbf{p},\mathbf{v})$ contains nonlinear coupling forces including Coriolis and centripetal accelerations. The vector $\mathbf{E}(\mathbf{p},\mathbf{v})$ is an additional vector which describes possibly nonconservative generalized forces and torques imparted on the system by the environment through which it moves.

The equations of motion for the five body ornithopter were derived using the presented equations and the software package Mathematica [16]. Although too lengthy to present, the resulting matrices are intuitive in their couplings and possess the expected properties [17]. For instance, the mass matrix is a symmetric positive definite matrix with the vehicle mass, vehicle inertia, and linkage inertia along the block diagonal, and terms representing couplings between the fuselage translational velocities, fuselage rotational velocities, and joint rates on the off diagonal. The mass matrix was partitioned by factoring the acceleration terms resulting from evaluating the first term in Eq. (8). The nonlinear coupling matrix does not have a unique representation, but by the extension of Lewis et al. [17], can be formulated as

$$\mathbf{C} = \frac{1}{2}\dot{\mathbf{M}} + \sum_{k=1}^{N}\left[\frac{\partial T}{\partial v_k}\right]\Gamma_k + \frac{1}{2}\left[\frac{\partial \mathbf{M}}{\partial \mathbf{p}}\right](\mathbf{v}\otimes\mathbb{I})(\mathbf{J}_K^{I,0}) - \frac{1}{2}(\mathbf{J}_K^{I,0})^T(\mathbb{I}\otimes\mathbf{v}^T)\left[\frac{\partial \mathbf{M}}{\partial \mathbf{p}}\right]^T \tag{12}$$

to guarantee properties used in passivity control, where $\mathbb{I}$ is the identity matrix and $\otimes$ is the Kronecker product operator [17,18]. The first contribution to the environmental effects vector $\mathbf{E}(\mathbf{p},\mathbf{v})$ is the resulting generalized force of gravity, which is found by differentiating the system potential energy and expressing the result in the reference frames of the generalized velocity states. The second contribution to this vector is the resulting generalized aerodynamic force generated by the motions of the wings and tail, which is currently not well known.

V. Preliminary Simulation Results

A simulation was performed for trimmed straight and level mean flight to illustrate resulting state trajectories. The ornithopter was initiated with an airspeed of 5 m/s. The wings were flapped at 4.7 Hz and the tail deflections were set to $\theta_{13} = -0.3491$ rad and $\theta_{23} = 0$ rad. An aerodynamics model for this ornithopter has not yet been identified; however, for preliminary results a simple quasi-steady thin airfoil model [19] was used for modeling lift and thrust on the wings as well as lift and drag on the tail. The aerodynamic coefficients and tail deflections were tuned to keep the ornithopter trimmed in steady mean flight.

Although controllable, the ornithopter is a highly underactuated system which only affords control over the flapping frequency of the wing joints θ_{11} and θ_{12}, and position of the tail joints θ_{13} and θ_{23}. In the absence of actuator models for the motors and drive mechanisms, a feedback linearization control law

$$\boldsymbol{\tau} = \mathbf{G}\mathbf{J}_K^{0,I}[\ddot{\mathbf{p}}_d - \dot{\mathbf{J}}_K^{I,0}\mathbf{v} + \mathbf{K}_P(\mathbf{p}_d - \mathbf{p}) + \mathbf{K}_D(\dot{\mathbf{p}}_d - \dot{\mathbf{p}})] + \mathbf{G}(\mathbf{C}\mathbf{v} + \mathbf{E}) \tag{13}$$

was used to synthetically maintain the sinusoidal wing stroke and the trimmed tail deflections for simulation purposes. The matrix $\mathbf{G}$ has the identity matrix along the lower block diagonal so that the control law is applied only to the linkage joints. The vector $\mathbf{p}_d$ is the desired position and has the prescribed joint trajectories in the last four elements. The terms $\mathbf{K}_P$ and $\mathbf{K}_D$ are positive definite matrices which regulate the tracking error in a proportional/derivative manner.

The simulated flight path of the fuselage center of mass is shown in Fig. 4, superimposed with silhouettes of the ornithopter configuration at several points in time. The longitudinal state trajectories are shown in Fig. 5, where the Euler pitch angle Θ is used to show the orientation. The lateral and directional states experienced small oscillations due to inertial couplings and offsets of the centers of mass, but these variations were many orders of magnitude less than corresponding longitudinal variables. There was a small drift in the longitudinal velocity, but otherwise the ornithopter was successfully trimmed for steady flight. The control law in Eq. (13) was successful in maintaining wing and tail trajectories, having position tracking errors on the order of 10^{-5} rad and velocity tracking errors on the order of 10^{-3} rad/s. Previous analysis of flight data [13] reported a 0.030-m amplitude oscillation in altitude, a 0.9-m/s amplitude oscillation in heave velocity, and a maximum 46.1-m/s^2 heave acceleration, whereas simulation produced results of 0.0290 m, 0.8693 m/s, and 23.0519 m/s^2, respectively. Additionally flight data reported a 0.1571-rad amplitude pitch angle oscillation and a 5.62-rad/s maximum pitch rate, whereas simulation produced results of 0.0560 rad and 1.8347 rad/s, respectively.

Comparing simulation to the flight data observations, the position states matched better than the velocity and acceleration states, and the translational states matched better than the rotational states. The largest source of error for these discrepancies is expected to be the aerodynamics model, which used quasi-steady approximations to describe what is known to be a highly unsteady flowfield [3,6,13]. Sources of error also stem from the rigid body assumptions, which neglect shape changes in the wings and flexibility in the fuselage and wing spars, uncertainties in the trim flight condition, and measurement errors in the inertial and geometric properties of the vehicle. However, despite the simplified aerodynamics model, the simulation was able to reproduce the trends observed in the flight data, indicating that the model captured the nonlinear and multibody interactions, and that an aerodynamics model should be identified for increased fidelity.

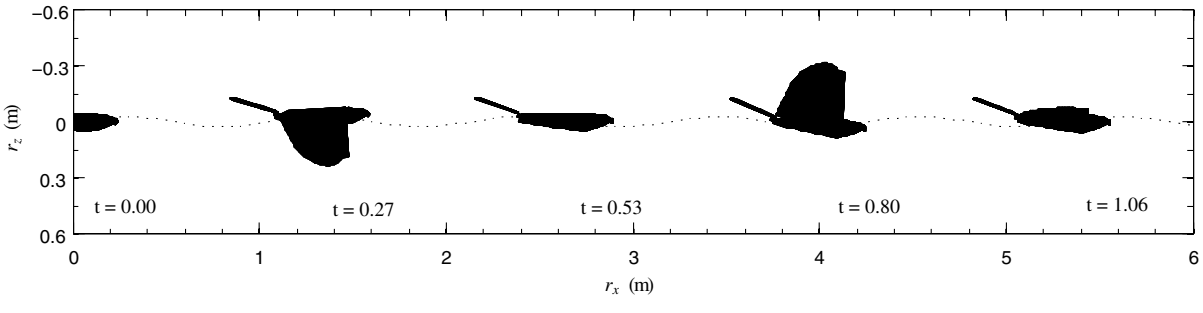

Fig. 4 Simulated flight path.

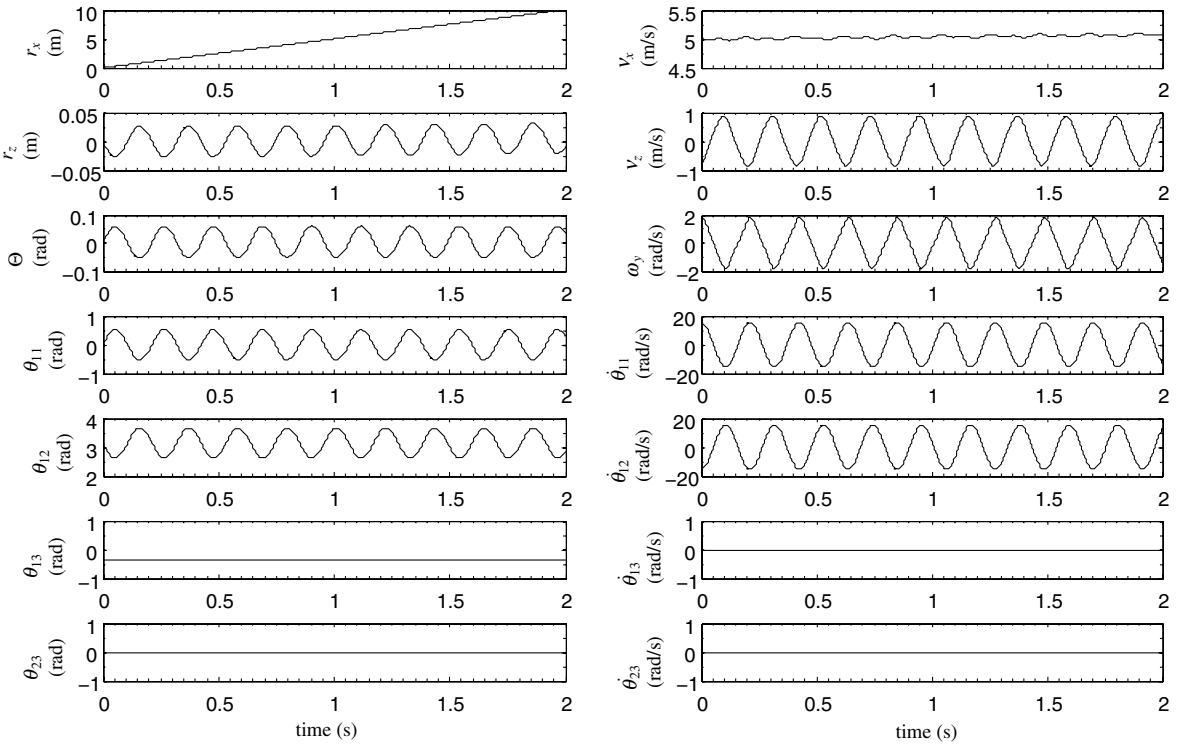

Fig. 5 Simulated state trajectories.

VI. Conclusions

This paper presented the derivation of the equations of motion for an ornithopter. Variations in the mass properties and observations of flight data warranted a nonlinear multibody model of the flight dynamics. Energy methods were used to derive the equations of motion, which were cast into a convenient form for system identification, nonlinear control, and simulation. A simplified aerodynamics model was used to simulate the system.

This paper argued that to meet the demand for an autonomous ornithopter flight platform with multimission capabilities such highly agile flight and perching maneuvers, a nonlinear multibody model of the flight dynamics must be developed. Justification for the modeling complexity stems from the fact that large and rapid variations in the mass properties occur, as well as the large flight envelope requisite for the envisioned maneuver capabilities.

The ornithopter equations of motion were cast into a canonical form used in the robotics and spacecraft communities. Unlike most robots and spacecraft, the ornithopter is a highly underactuated system; however, representing the ornithopter in this form begins to bridge a gap to a wealth of information on nonlinear control and adaptive system identification of mechanical systems. Additionally this canonical form is convenient for system identification and simulation, can be augmented easily for different aircraft configurations, and has a minimal number of state equations with known properties.

A quasi-steady thin airfoil model of the aerodynamics was used to simulate straight and level mean flight. Although parameters were tuned and it is known that the aerodynamic flowfield is highly unsteady, the simulation appears realistic and was able to capture general trends measured previously in flight data. This result indicates the need to identify a more realistic aerodynamics model and provides further justification for the nonlinear multibody modeling of the flight dynamics.

Acknowledgments

The authors would like to thank the University of Maryland, The National Institute of Aerospace, and the NASA Langley Research Center for their support in this research. Several discussions with Robert Sanner and Sean Humbert are acknowledged and appreciated. The authors would also like to thank the members of the Morpheus Laboratory for their continued teamwork and motivation, with additional thanks to Nelson Guerreiro for creating the visualization environment used in the simulation.

References

[1] Sane, S., and Dickinson, M., "The Aerodynamic Effects of Wing Rotation and a Revised Quasi-Steady Model of Flapping Flight," *Journal of Experimental Biology*, Vol. 205, No. 8, April 2002, pp. 1087–1096.

[2] DeLaurier, J., "An Aerodynamic Model for Flapping-Wing Flight," *Journal of the Royal Aeronautical Society*, Vol. 97, April 1993, pp. 125–130.

[3] Harmon, R., Grauer, J., Hubbard, J., and Humbert, S., "Experimental Determination of Ornithopter Membrane Wing Shapes Used for Simple Aerodynamic Modeling," AIAA Paper No. 2008-6397, Aug. 2008.

[4] Vest, M., and Katz, J., "Unsteady Aerodynamic Model of Flapping Wings," *AIAA Journal*, Vol. 34, No. 7, July 1996, pp. 1435–1440. doi:10.2514/3.13250

[5] Bush, B., and Baeder, J., "Force Production Mechanisms of a Flapping MAV Wing," *AHS International Specialists' Conference on Aeromechanics*, American Helicopter Society, Alexandria, VA, Jan. 2009.

[6] Roget, B., Sitaraman, J., Harmon, R., Grauer, J., Conory, J., Hubbard, J., and Humbert, S., "A Computational Study of Flexible Wing Ornithopter Flight," AIAA Paper No. 2008-6397, Aug. 2008.

[7] Taylor, G., and Thomas, A., "Dynamic Flight Stability in the Desert Locust Schistocerca Gregaria," *Journal of Experimental Biology*, Vol. 206, No. 16, 2003, pp. 2803–2829. doi:10.1242/jeb.00501

[8] Deng, X., Schenato, L., Wu, W., and Sastry, S., "Flapping Flight for Biomimetic Robotic Insects: Part 1—System Modeling," *IEEE Transactions on Robotics and Automation*, Vol. 22, No. 4, Aug. 2006, pp. 776–788.

[9] Sibilski, K., "Dynamics of Micro-Air-Vehicle with Flapping Wings," *Acta Polytechnica*, Vol. 44, No. 2, 2004, pp. 15–21.

[10] Wu, J., and Popović, Z., "Realistic Modeling of Bird Flight Animations," *ACM Transactions on Graphics*, Vol. 22, No. 3, July 2003, pp. 888–895. doi:10.1145/882262.882360

[11] Rashid, T., "The Flight Dynamics of a Full-Scale Ornithopter," M.S. Thesis, University of Toronto, 1995.

[12] Kinkade, S., "Hobby Technik," www.appingight.com, 2008.

[13] Grauer, J., and Hubbard, J., "Inertial Measurements from Flight Data of a Flapping-Wing Ornithopter," *Journal of Guidance, Control, and Dynamics*, Vol. 32, No. 1, Jan.–Feb. 2009, pp. 326–331. doi:10.2514/1.37495

[14] Slotine, J., and Li, W., *Applied Nonlinear Control*, Prentice–Hall, Englewood Cliffs, NY, 1991.

[15] Sanner, R., and Essex, C., "Multiresolution Radial Basis Function Networks for the Adaptive Control of Robotic Systems," *UKACC International Conference on Control '96*, Conf. Publ. No. 427, Vol. 2, IEEE, Piscataway, NJ, Sept. 1996, pp. 894–898.

[16] Wolfram Research, "Mathematica," www.wolfram.com., 2008.

[17] Lewis, F., Dawson, D., and Abdallah, C., *Robot Manipulator Control*, 2nd ed., Control Engineering Series, Marcel Dekker, New York, 2004, pp. 107–221.

[18] Brewer, J., "Kronecker Products and Matrix Calculus in System Theory," *IEEE Transactions on Circuits and Systems*, Vol. 25, No. 9, 1978, pp. 772–781. doi:10.1109/TCS.1978.1084534

[19] Leishman, J., *Principles of Helicopter Aerodynamics*, 2nd ed., Cambridge Aerospace, Cambridge University Press, New York, 2006, pp. 423–524.